Journal of Orthodontic and Periodontal Biomaterials Research

2025, Volume 5, Issue 1, Page No: 93-102

Available online at: https://galaxypub.co/

Galaxy Publication

Impact of Force Control Strategies on the Stability of Orthodontic Mini-Implants

Kofi V. Mokoena[1], Amina U. Mensah[1]*, Fatou Mokoena[2], Grace Nkosi[2], Kofi Ndiaye[1]

[1]Department of Orthodontics and Dentofacial Orthopedics, College of Dental Medicine, University of Cape Town, Cape Town, Cameroon.
[2]Department of Dental Public Health, School of Medicine and Dentistry, Makerere University, Kampala, Kenya.

***E-mail** ✉ amina.mensah@hotmail.com

Received: 11 March 2025; **Revised:** 17 June 2025; **Accepted:** 23 June 2025

ABSTRACT

This investigation explores the biomechanical response of titanium mini-implants (Ti6Al4V) subjected to various orthodontic loading conditions using finite element analysis (FEA). The purpose is to assess their strength, fatigue resistance, and structural reliability under clinically relevant forces. Appropriate force magnitudes are essential for maintaining implant durability and preventing deleterious stress transmission to surrounding bone tissues. A standard titanium MI (2.0 mm in diameter, 12 mm in length) was modeled and analyzed in an FEA framework. The mandibular structure was reconstructed from computed tomography (CT) data using SpaceClaim 2023.1 and meshed into 10-node tetrahedral elements in ANSYS Workbench. Material constants were defined based on published data, and the bone–implant interface was simulated through a nonlinear frictional contact model. Orthodontic loads of 2 N and 10 N, each applied at a 30° inclination, were tested to replicate actual treatment conditions. Mechanical outputs—including total deformation, von Mises stress, equivalent strain, fatigue life, and safety factors—were examined to evaluate overall implant performance. At a load of 2 N, displacement was minimal (0.0328 mm), and the model sustained approximately 445,000 loading cycles within safe fatigue limits, maintaining a safety factor of 4.8369. Under a 10 N load, however, the implant endured only 1546 cycles before predicted failure, accompanied by increased stress (6.468×10^5 MPa) and concentrated strain zones—suggesting a higher likelihood of structural failure and bone overload. The simulations identified a force threshold beyond which mechanical stability and peri-implant health deteriorate. Findings confirm that maintaining orthodontic forces near 2 N maximizes implant lifespan and preserves bone integrity. Conversely, excessive loads (around 10 N) drastically shorten service life and raise the risk of mechanical or biological complications. These outcomes underscore the importance of carefully calibrated force application to enhance the efficiency and longevity of orthodontic mini-implants.

Keywords: Cortical bone, Finite element modelling, Fatigue, Mini-Implant, Orthodontic load, Stress response

How to Cite This Article: Mokoena KV, Mensah AU, Mokoena F, Nkosi G, Ndiaye K. Impact of Force Control Strategies on the Stability of Orthodontic Mini-Implants. J Orthod Periodontal Biomater Res. 2025;5(1):93-102. https://doi.org/10.51847/UpKL9nJfM0

Introduction

Orthodontic mini-implants (MIs) are widely used as temporary anchorage devices (TADs) due to their reliable support during tooth movement. Nevertheless, their reported failure rates—ranging from 5% to 30%—remain a clinical concern, influenced by anatomical site, patient-specific variables, and loading intensity [1–4]. A primary factor in these failures is inadequate primary stability, which determines how effectively the implant maintains mechanical engagement with surrounding bone under orthodontic stress [5, 6].

Among several determinants, cortical bone thickness at the placement site plays a crucial role. Studies indicate that the anterior palate provides higher success rates than buccal or interradicular regions [7]. However, how cortical thickness affects MI success under differing orthodontic forces is still insufficiently documented. This knowledge gap is significant because thin cortical regions can experience localized stress peaks, resulting in microfractures, implant loosening, or even treatment failure [8, 9].

Cortical bone acts as the principal load-bearing structure distributing stress during tooth movement. While previous research links thinner cortical areas to increased stress levels, their exact impact on implant stability and remodeling mechanisms remains uncertain [8]. In TAD-related contexts, the interaction between implant geometry, insertion angle, and bone density must be optimized to ensure mechanical retention [10–12].

Recent technological advances—such as three-dimensional simulations, finite element analysis (FEA), and novel biomaterials—enable a more accurate evaluation of stress and strain fields around implants [13–18]. These innovations contribute to individualized treatment planning and more predictable clinical results. For instance, studies suggest that inserting MIs at an oblique angle reduces cortical stress and may lower the incidence of mechanical failure [4, 19]. Moreover, titanium alloys whose mechanical properties closely resemble natural bone can lessen stress-shielding and improve load transfer [20, 21].

Despite such progress, comprehensive evaluations addressing the combined effects of cortical bone thickness, orthodontic force magnitude, and MI stability are lacking. This study addresses that deficiency by systematically analyzing how variations in cortical bone support influence mechanical stress patterns and implant reliability. Employing FEA, this research aims to generate data-driven recommendations for optimizing MI design and placement, thereby improving current orthodontic practice. Maintaining orthodontic forces within an optimal range remains fundamental for extending implant longevity and safeguarding peri-implant bone health.

Materials and Methods

Geometric modeling

In this analysis, a titanium mini-implant (Ti6Al4V; Jeil Medical Corporation, Seoul, South Korea) with a 2.0 mm diameter and 12 mm length was digitally replicated through finite element modeling (FEM) **(Figure 1a)**. The mandibular geometry was acquired from computed tomography (CT) scans (DEXIS, Biberach, Germany), which were subsequently digitized for use in the modeling process **(Figure 1b)**. Three-dimensional representations of both the implant and mandible were reconstructed and integrated within the SpaceClaim 2023.1 CAD environment to create a complete assembly **(Figure 1c)**.

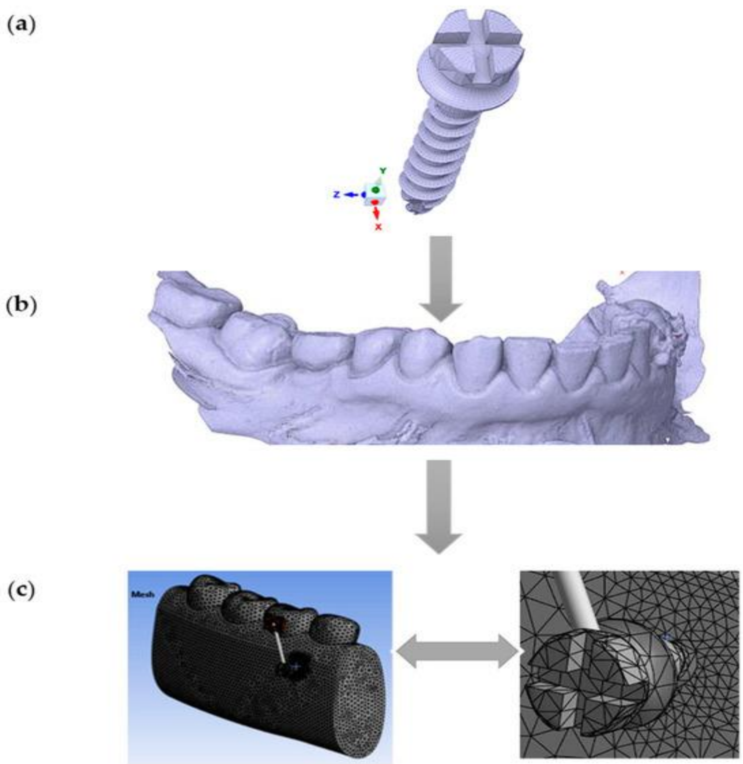

Figure 1. Workflow illustrating the finite element modeling process for the orthodontic MI and its adjacent bone structures: (a) commercial Ti implant (2 mm diameter) represented via FEM; (b) mandible geometry derived from CT data (STL format); (c) complete 3D model meshed into finite elements (left) and magnified section displaying the MI region and the surrounding anchorage zone (right)

Simulation Parameters

The implant insertion site was defined between the premolar and molar region. The assembled model was imported into ANSYS Workbench 2021 (ANSYS Inc., Canonsburg, PA, USA) and discretized using 10-node tetrahedral structural elements. The MI, cortical and cancellous bone, teeth, and periodontal ligament were all simulated as linearly elastic, homogeneous, and isotropic materials. Mechanical constants for each material were adopted from previously published literature **(Table 1)**.

Interfaces between the tooth and periodontal ligament were modeled as perfectly bonded, while the MI–bone interface was treated as a nonlinear frictional contact (friction coefficient = 0).

Table 1. Mechanical characteristics applied in the finite element model, derived from validated references to ensure simulation accuracy [22]

Element	Rigidity (MPa)	Strain Ratio
Bracket	380,000	0.19
Mini-Implant	110,000/200,000	0.3
Tooth	84,100	0.2
PDL	68.9	0.45
Cortical Bone	17,000	0.3
Spongy Bone	350	0.25

To recreate clinical orthodontic loading, forces of 2 N and 10 N were applied at a 30° inclination relative to the vertical (Y) axis. The loads were directed from the implant head toward the molar via a connector tube, accurately simulating a molar intrusion scenario under skeletal anchorage. This oblique force configuration replicates stress transfer patterns observed in practice, enabling a realistic evaluation of strain and stress distributions within the periodontal ligament, alveolar bone, and nearby tissues.

Technical details of FEA modeling

Table 2 summarizes the computational setup used for finite element analysis (FEA). The principal parameters of the simulation framework are described below.

Table 2. Parameters of the finite element model

Parameter	Details
Mesh Discretization	356,422 nodes / 229,672 elements
Element Type	10-node tetrahedral
Analysis Software	ANSYS Workbench 19.2, Canonsburg, PA, USA
Material Behavior	Linear, isotropic, uniform
Contact Behavior	Nonlinear friction (coefficient = 0 between mini-implant and bone), bonded (linear)
Applied Load	Oblique forces (0.1–10 N) at angles of 30°, 45°, 60°
Mini-Implant Design	Threaded, 2.0 mm diameter, 12.0 mm length
Boundary Constraints	Full osseointegration (100%)

1. **Discretization (nodes/elements):** Indicates the total number of elements and nodes defining the mesh. A denser mesh corresponds to greater geometrical precision and more accurate mechanical interaction results.
2. **Element:** The model employed 10-node tetrahedral elements for discretization, allowing fine resolution of complex surfaces and internal stress fields.
3. **Software:** Finite element simulations were carried out using ANSYS software.
4. **Material model:** Materials were treated as isotropic, uniform, and linearly elastic, ensuring direction-independent behavior under loading.
5. **Contact model:** A nonlinear frictional formulation defined interactions between the MI and surrounding bone, while **bonded constraints** represented other interfacial contacts.
6. **Loading:** The applied forces were **oblique**, varying between 2 N and 10 N, to emulate orthodontic stress conditions.

7. **MI type:** The simulated implant corresponded to **a** threaded titanium device measuring 2 mm in diameter **and** 12 mm in length**.**
8. **Boundary conditions:** Full osseointegration (100%) was assumed, implying rigid fixation between the MI and bone without any interfacial displacement.

Results and Discussion

Static structural simulations were conducted under the assumption of an undamped mechanical system, excluding heterogeneity in material response. The elastic isotropic stiffness model was employed for all components. The primary outcomes for the 2 N loading condition are summarized below.
The MI was embedded 7 mm deep within the bone and subjected to a 30° oblique orthodontic load relative to the vertical (Y) axis. The implant was positioned perpendicular (90°) to both cortical and cancellous bone surfaces during insertion.

Measurements: Overall deformation, von mises stress, and equivalent strain
The finite element simulation (FEM) was utilized to interpret the mechanical response of the mini-implant (MI) under orthodontic force application, emphasizing the analysis of total displacement, stress distribution, and strain levels. According to **Figure 2a**, the largest displacement (0.032799 mm) appeared at the tip of the implant where the external force was applied. This pattern arises naturally because the threaded part is firmly anchored, while bending forces cause the greatest movement at the upper free region. The von Mises stress field in **Figure 2b** revealed a maximum stress of 99.237 MPa, concentrated within the screw threads—an area that commonly exhibits mechanical failure. This stress concentration indicates a possible fatigue origin under repetitive loading. The equivalent strain map **(Figure 2c)** identified the maximum strain value as 0.00090338, again focused in the threaded zone. The alignment of peak stress and strain demonstrates that this area is most vulnerable to mechanical deterioration over extended use.

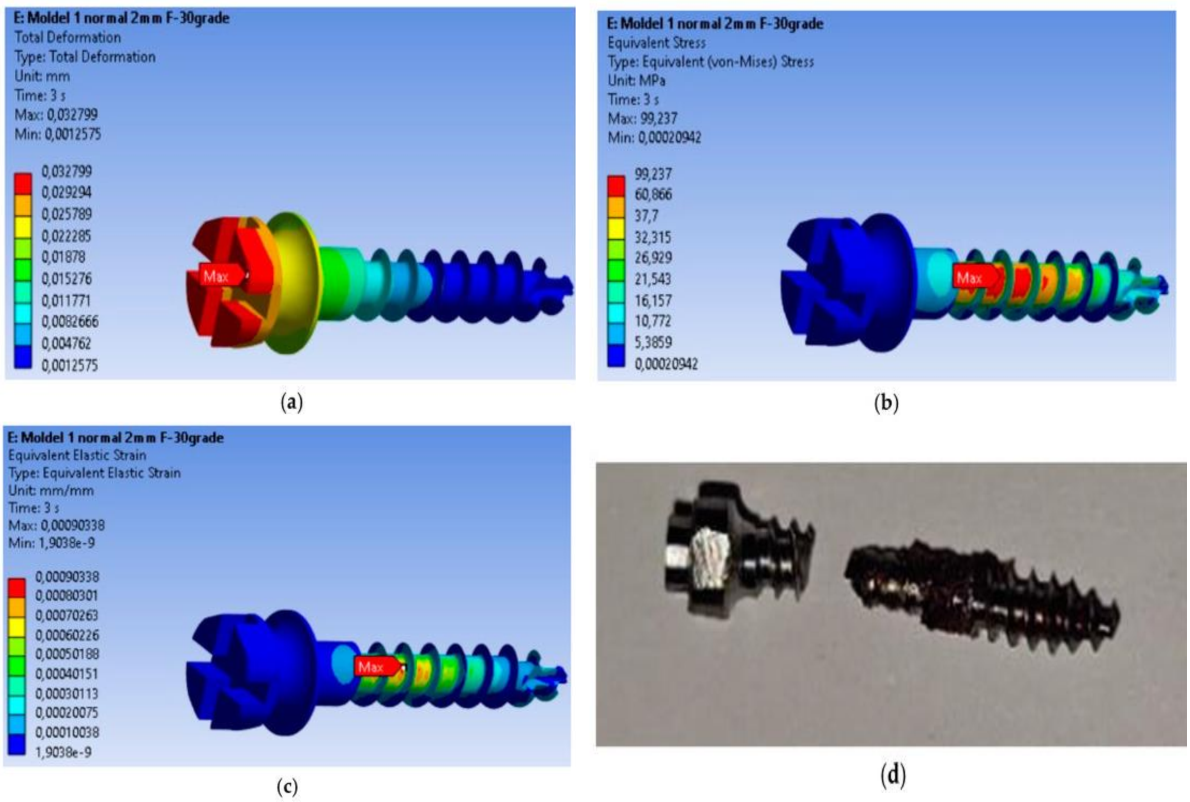

Figure 2. Finite element simulation of an MI under 2 N oblique load at 30°: (a) Overall deformation; (b) von Mises stress field; (c) Equivalent strain; (d) Physical breakage after removal observed at the stress-concentrated zone predicted by FEM

The experimental evidence in **Figure 2d** confirms the computational findings, showing that the implant fractured exactly where the numerical model indicated the highest stress intensity. This match between prediction and observation validates the FEM approach and supports its accuracy in mapping deformation and stress behavior.

Structural safety evaluation: factor of safety, safety margin, and stress ratio
The distribution of safety factors for the implant is shown in **Figure 3a**. The lowest recorded value, 4.8369, corresponds to the node experiencing the greatest stress intensity, confirming that the component satisfies the mechanical resistance limits. These data were generated for a 2 N orthodontic load. The safety factor was obtained as the ratio of material yield strength (480 MPa)—measured experimentally for titanium—to the computed von Mises stress. The safety margin results are presented in **Figure 3b**, with the minimum margin recorded at 3.8369.

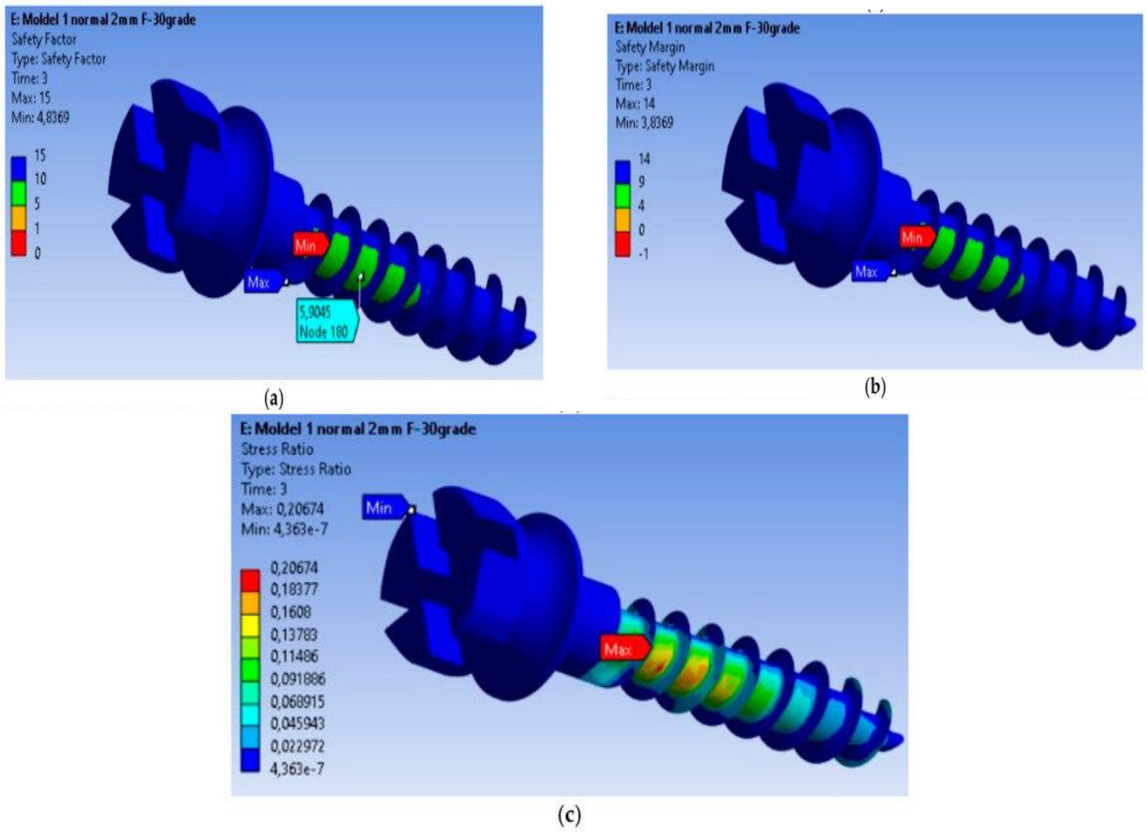

Figure 3. MI safety performance under 2 N orthodontic load: (a) Safety factor σc/σMax; (b) Safety margin (σc/σMax − 1); (c) Stress ratio σMax/σc

From **Figure 3c**, the stress ratio—representing the ratio between simulated stress and yield strength—reaches its maximum value of 0.20674, again observed at the point of maximum equivalent stress.

Fatigue resistance under 2 N orthodontic loading: Service life, factor of safety, and failure estimation
A fatigue study was carried out following a symmetric alternating stress condition, in accordance with the ASME elliptical model [23]. The fatigue life was estimated using the von Mises equivalent stress, applying a scaling coefficient of 1. The outcomes reveal that the MI can function effectively for approximately 4.445×10^5 cycles without structural defects when subjected to a 2 N orthodontic load. As illustrated in **Figure 4a–c**, this minimum life corresponds to a minor region of the implant, while most of the remaining volume shows endurance levels near 10^6 cycles. The highest computed value (2250) was obtained for the node where the lowest fatigue life occurred, around 2.5 times higher than surrounding areas. The minimum fatigue safety factor—shown in **Figure 4c**—was 0.86863, detected at the region of maximum stress accumulation.

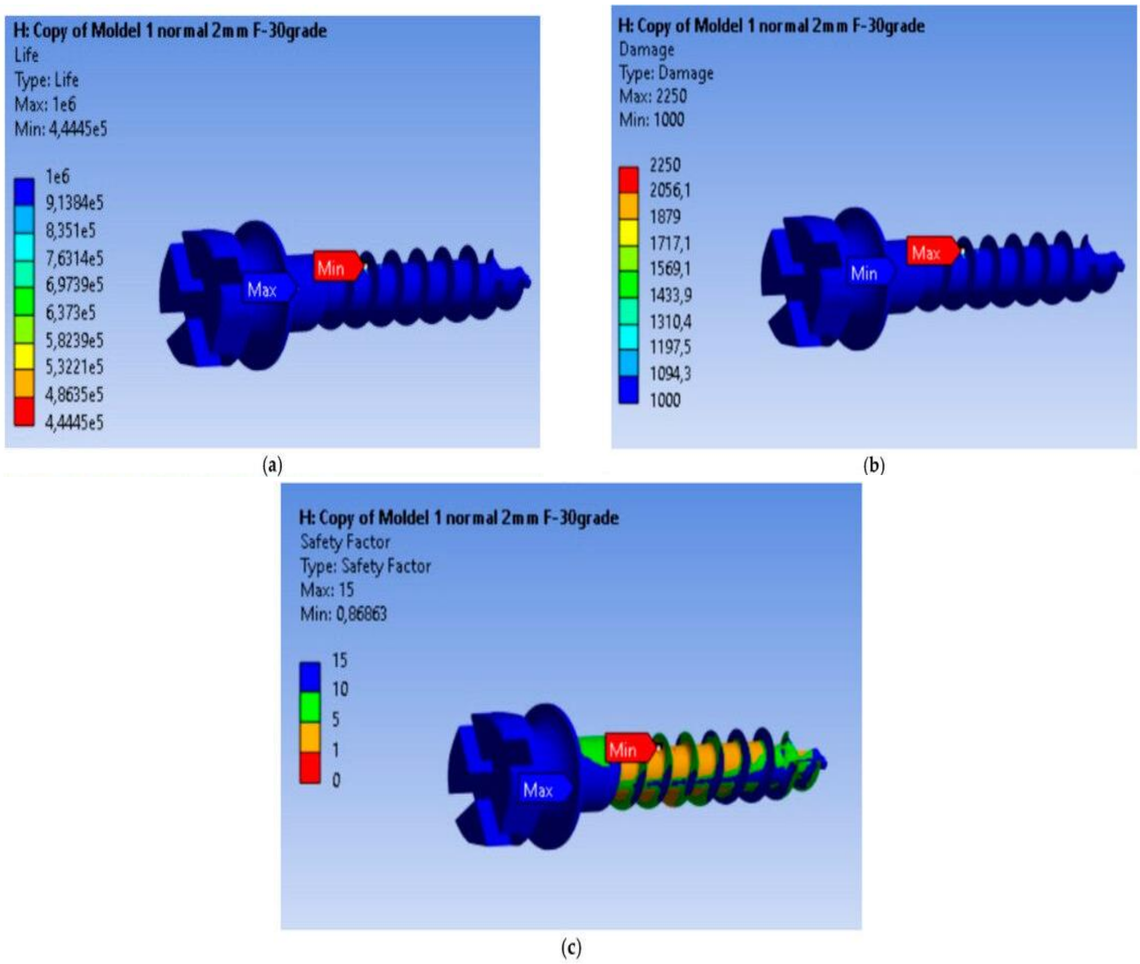

Figure 4. Durability evaluation of MI under 2 N applied force: (a) Fatigue life distribution; (b) Failure probability; (c) Fatigue safety factor map

Fatigue behavior of the MI under 10 N load: Lifespan, safety evaluation, and failure assessment

The predicted durability of the mini-implant (MI) when subjected to a 10 N orthodontic force is displayed in **Figure 5a**. The simulation indicates that the implant can operate without mechanical failure for only 1546 cycles, which is approximately 287.48 times shorter than the lifespan observed under a 2 N load. This demonstrates a sharp reduction in service life when the applied force increases. **Figure 5b** illustrates the failure distribution, showing a maximum stress of 6.468 × 10^5 MPa at the node with the lowest fatigue life, which is 6.468 × 10^2 times higher than stress in the remaining material. The minimum fatigue safety factor measured at this location is 0.17704, as shown in **Figure 5c**, indicating high vulnerability under this load condition.

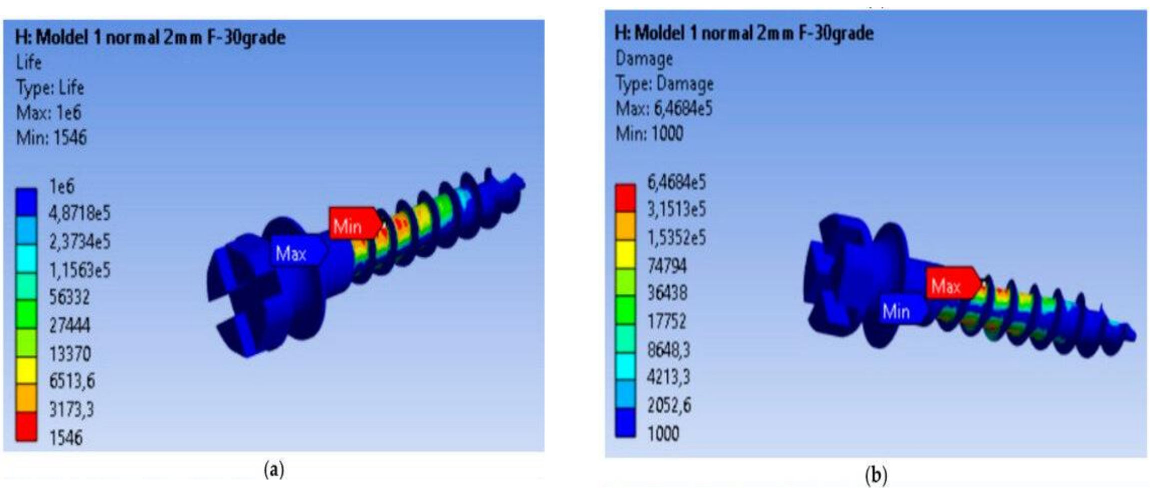

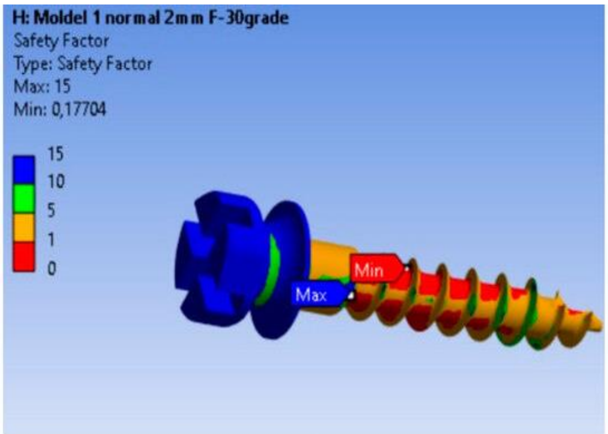

(c)

Figure 5. Fatigue assessment of the MI with 10 N applied force: (a) Predicted lifespan; (b) Failure magnitude; (c) Fatigue safety factors

In comparison with the 2 N case **(Table 3)**, the 10 N load drastically shortens the implant's functional life, subjects a larger portion of the material to critical stress, and reduces the fatigue safety factor. These findings underscore the necessity of applying clinically appropriate forces to maximize the longevity of orthodontic implants.

Table 3. Effect of 2 N vs. 10 N forces on mini-implant performance

Metric	2 N Load	10 N Load
Durability (cycles)	4.445 × 10^5 cycles	1546 cycles (287.48 times lower)
Affected Material Volume	Limited material volume	Expanded material volume
Lowest Fatigue Safety Factor	0.86863 (at highest stress point)	0.17704 (at highest stress point)
Peak Stress Intensity	2250 MPa (2.5× greater than other regions)	6.468 × 10^5 MPa (646.8× greater than other regions)

Defining deformation limits for orthodontic mini-implants is essential to maintain their mechanical stability and operational lifespan during treatment. Understanding the elements that influence these limits is crucial for safe and effective clinical use.

Applying a 2 N orthodontic force is generally considered optimal in practice, as it provides adequate stability for controlled tooth movement while minimizing the risk of structural compromise. Literature indicates that forces within the 1.5–2.5 N range are commonly applied in procedures such as canine retraction [24], aligning with safe limits for immediate loading of MIs [4]. The stress distribution surrounding an MI is highly dependent on the magnitude of the applied force and the mechanical properties of the adjacent bone, as demonstrated by finite element studies [25]. While MIs tolerate immediate loading safely, excessive forces may provoke displacement, deformation, or failure [26].

Finite element analysis (FEA) offers a powerful method for anticipating the mechanical behavior of implants under various loading scenarios. The accuracy of FEA results is strongly influenced by modeling assumptions. For example, assuming full osseointegration (100%) simplifies computations but does not reflect biological variability, potentially causing deviations in predicted stress concentrations, load transfer, and failure zones [27].

Analysis of displacement, stress, strain, and safety factors in mini-implants

Displacement: The maximum total displacement of 0.032799 mm at the MI tip indicates a concentrated bending effect, critical for evaluating end deflection under orthodontic forces.

Stress: The peak von Mises stress of 99.237 MPa occurs in the threaded region, signifying the probable site for mechanical failure. Design strategies should focus on strengthening this area to improve fatigue resistance.

Equivalent strain: The maximum equivalent strain of 0.00090338, also concentrated in the threads, provides a measure of material deformation and highlights regions requiring attention in implant design and material selection to reduce deformation and improve stability.

Safety factors: The minimum safety factor shows that the MI meets mechanical requirements and can withstand the applied orthodontic forces without significant risk of fracture or excessive deformation.

Stress ratio and fatigue behavior of the mini-implant

The stress ratio, calculated by dividing the stress experienced by the MI by the yield strength of its titanium material, provides essential information about how close the implant is to reaching its mechanical limits. This value is crucial for understanding the safety margins and ensuring that applied orthodontic loads do not exceed structural tolerance. The highest stress ratio occurs at the same nodes where the von Mises stress peaks, identifying critical points that may compromise implant stability.

Fatigue assessment indicates that the primary failure location is concentrated at a specific node with the lowest fatigue life, revealing a vulnerable spot within the implant. This insight can inform future design optimizations to enhance durability. Under normal orthodontic forces of 2 N, the MI is expected to function safely for roughly 4.445×10^5 cycles, demonstrating high reliability. However, exposure to increased forces greatly heightens susceptibility to mechanical damage, restricting the safe application of higher loads. Fatigue safety factors in such conditions show a pronounced reduction, highlighting the potential for structural failure.

These observations stress the importance of matching orthodontic force magnitudes to the mechanical limitations of each MI, reducing the risk of fractures or bone damage. Studies, such as those by Nienkemper *et al.,* also point out that loading duration impacts implant displacement, showing that both the magnitude and time of force application determine the mechanical response [26]. Clinically, recommended forces for MIs usually range between 3.75 and 4.5 N to maintain optimal anchorage without overloading the implant [25].

Future research opportunities

The results suggest several directions for continued research, aimed at improving MI longevity and clinical performance. Potential studies could include advanced simulation models **or** experimental testing to verify mechanical predictions and refine implant design, insertion techniques, and force protocols.

Limitations of the current study

1. **Implant length restriction:** Only **12 mm MIs** were evaluated, limiting understanding of the effects of varying lengths on mechanical performance. Future research should examine multiple sizes.
2. **Bone model simplifications:** Cortical and cancellous bone were modeled as **linear, isotropic, and elastic**, which does not fully replicate the complex properties of real bone tissue.
3. **Material scope:** Analysis was restricted to **Ti6Al4V**, without comparison to other metals like **316L stainless steel**, which could influence fatigue performance and clinical outcomes.
4. **Idealized conditions:** The study assumed **perfect insertion and complete osseointegration (100%)**, whereas clinical conditions often vary, potentially altering implant stability and stress distribution.

Conclusion

This investigation underscores the necessity of maintaining orthodontic forces near 2 N to preserve both the structural integrity of MIs and the health of surrounding bone. Under 2 N loading, finite element analysis predicts approximately 445,000 safe cycles, with stress and strain levels within acceptable limits. By contrast, 10 N loading reduces implant lifespan dramatically to 1546 cycles, with stress and strain levels rising sharply, increasing the likelihood of implant failure and damage to adjacent bone, particularly cortical bone near the anchorage.

The study highlights that careful regulation of applied forces is critical for optimizing MI performance, preventing complications, and ensuring long-term clinical success. Adhering to controlled loading conditions allows clinicians to maximize MI lifespan while safeguarding peri-implant bone integrity.

Acknowledgments: None

Conflict of interest: None

Financial support: None

Ethics statement: None

References

1. Malik F, Khan F, Ali S, Rana F, Haq H, Hussain M. Factors affecting success and failure of orthodontic mini-implants: A retrospective review. Prof Med J. 2023;30:285–91.
2. Ravi J, Duraisamy S, Rajaram K, Kannan R, Arumugam E. Survival rate and stability of surface-treated and non-surface-treated orthodontic mini-implants: A randomized clinical trial. Dent Press J Orthod. 2023;28:e2321345.
3. Jeong J, Kim J, Lee N, Kim Y, Lee J, Kim T. Analysis of time to failure of orthodontic mini-implants after insertion or loading. J Korean Assoc Oral Maxillofac Surg. 2015;41:240–5.
4. Popa A, Dehelean C, Călniceanu H, Watz C, Brad S, Sinescu C, Szuhanek C. A custom-made orthodontic mini-implant—Effect of insertion angle and cortical bone thickness on stress distribution with a complex in vitro and in vivo biosafety profile. Materials. 2020;13:4789.
5. Singh J, Singh S, Gupta A. Comparative evaluation of primary stability of two different types of orthodontic mini-implants. J Pharm Bioallied Sci. 2021;13:128–35.
6. Dutta S, Bhat J. Orthodontic mini implant and their primary stability: A comparative study. Int J Appl Dent Sci. 2022;8:642–4.
7. Arqub SA, Gandhi V, Mehta S, Palo L, Upadhyay M, Yadav S. Survival estimates and risk factors for failure of palatal and buccal mini-implants. Angle Orthod. 2021;91:756–63.
8. Filipová D, Filipi V, Kamínek M. Proclination-induced changes in the labial cortical bone thickness of lower incisors. Bratisl Med J. 2019;120:155–60.
9. Kovuru V. Factorial analysis of variables affecting bone stress adjacent to mini-implants used for molar distalization by direct anchorage—A finite element study. J Orthod Sci. 2023;12:18.
10. Son E, Kim S, Hong C, Chan V, Sim H, Ji S, Chae H. A study on the morphologic change of palatal alveolar bone shape after intrusion and retraction of maxillary incisors. Sci Rep. 2020;10:14454.
11. Thongudomporn U, Charoemratrote C, Jearapongpakorn S. Changes of anterior maxillary alveolar bone thickness following incisor proclination and extrusion. Angle Orthod. 2014;85:549–54.
12. Pan C, Liu P, Tseng Y, Chou S, Wu C, Chang H. Effects of cortical bone thickness and trabecular bone density on primary stability of orthodontic mini-implants. J Dent Sci. 2019;14:383–8.
13. Yu W, Tsai M, Yu J, Huang H, Hsu J. Bone quality affects stability of orthodontic miniscrews. Sci Rep. 2022;12:2849.
14. Centeno A, Fensterseifer C, Chami V, Ferreira E, Marquezan M, Ferrazzo V. Correlation between cortical bone thickness at mini-implant insertion sites and age of patient. Dent Press J Orthod. 2022;27:e222098.
15. Marquezan M, Mattos C, Sant'Anna E, Souza M, Maia L. Does cortical thickness influence the primary stability of miniscrews? A systematic review and meta-analysis. Angle Orthod. 2014;84:1093–103.
16. Hatia A, Doldo T, Parrini S, Chisci E, Cipriani L, Montagna L, et al. Accuracy and completeness of ChatGPT-generated information on interceptive orthodontics: A multicenter collaborative study. J Clin Med. 2024;27:735.
17. Sant'Anna EF, Araújo MTS, Nojima LI, Cunha ACD, Silveira BLD, Marquezan M. High-intensity laser application in orthodontics. Dent Press J Orthod. 2017;22:99–109.
18. Weir T. Clear aligners in orthodontic treatment. Aust Dent J. 2017;62(Suppl 1):58–62.
19. Rito-Macedo F, Barroso-Oliveira M, Paranhos LR, Rodrigues-Brum J, Pereira-Lima IF, Gomes-França FM, de Brito-Junior RB. Implant insertion angle and depth: Peri-implant bone stress analysis by the finite element method. J Clin Exp Dent. 2021;10:1167–73.
20. Panaite T, Savin C, Olteanu ND, Karvelas N, Romanec C, Vieriu RM, et al. Heat treatment's vital role: Elevating orthodontic mini-implants for superior performance and longevity—Pilot study. Dent J. 2024;12:103.
21. Cozzani M, Pasini M, Zallio F, Ritucci R, Mutinelli S, Mazzotta L, et al. Comparison of maxillary molar distalization with an implant-supported distal jet and a traditional tooth-supported distal jet appliance. Int J Dent. 2014;10:1–7.
22. Benaissa A, Merdji A, Bendjaballah MZ, Ngan P, Mukdadi OM. Stress influence on orthodontic system components under simulated treatment loadings. Comput Methods Programs Biomed. 2020;195:105743.
23. ASME Elliptical. Available from: https://www.asme.org/. Accessed 2024 Jun 1.

24. Ghorab H. Finite element study to evaluate the stress around mini-implant during canine retraction using continuous and interrupted orthodontic forces. Open Access Maced J Med Sci. 2023;11:36–43.
25. Alrbata R, Momani M, Al-Tarawneh A, Ihyasat A. Optimal force magnitude loaded to orthodontic microimplants: A finite element analysis. Angle Orthod. 2015;86:221–6.
26. Nienkemper M, Handschel J, Drescher D. Systematic review of mini-implant displacement under orthodontic loading. Int J Oral Sci. 2013;6:1–6.
27. Klein CP, van der Waerden J. The effect of osseointegration on the mechanical stability of dental implants: A finite element analysis. J Biomech. 2015;48:1–7.